NBSIR 86-3063

# FAR-FIELD TRANSIENT RESPONSE OF AN ANTENNA FROM NEAR-FIELD DATA

David A. Hill

National Bureau of Standards
U.S. Department of Commerce
Boulder, Colorado 80303

December 1986

NBSIR 86-3063

# FAR-FIELD TRANSIENT RESPONSE OF AN ANTENNA FROM NEAR-FIELD DATA

David A. Hill

Electromagnetic Fields Division
Center for Electronics and Electrical Engineering
National Engineering Laboratory
National Bureau of Standards
Boulder, Colorado 80303

December 1986

Sponsored by
Defense Nuclear Agency
Alexandria, Virginia 22310

U.S. DEPARTMENT OF COMMERCE, Malcolm Baldrige, Secretary

NATIONAL BUREAU OF STANDARDS, Ernest Ambler, Director

CONTENTS

**FAR-FIELD TRANSIENT RESPONSE OF AN ANTENNA FROM NEAR-FIELD DATA**

David A. Hill

Electromagnetic Fields Division
National Bureau of Standards
Boulder, CO 80303

The theory for calculating the transient far-field response of an antenna from planar near-field data in either the time domain or the frequency domain has been developed. A double integral must be evaluated if we begin with time-domain data, but a triple integral must be evaluated if we begin with frequency-domain data. However, the frequency-domain integrals are in a form that is suitable for three-dimensional FFT. Two idealized examples are studied, and identical results are obtained starting with frequency-domain or time-domain data. The main practical difficulty in determining the transient response is the large number of near-field samples that are required. If data are taken at only a few near-field points, then the singularity expansion method (SEM) presents a possible method of determining the complex resonances of the antenna under test.

Key words: antenna; complex resonance; far field; frequency domain; near field; singularity expansion method (SEM); time domain.

## 1. INTRODUCTION

The response of antennas to out-of-band frequencies [1-4] plays an important role in interference and jamming problems. Earlier work in this area at the National Bureau of Standards (NBS) included an analysis of reflector antennas [5] and an analysis and near-field measurements of antenna arrays [6].

This earlier work applied to single-frequency cw signals, but many interfering signals, such as high-power microwaves (HPM), are actually pulsed signals with a fairly complicated time dependence. Thus it would be useful to be able to determine the transient response of antennas illuminated by pulsed signals. The transient far-field patterns of HPM sources are also difficult to determine because it is generally difficult to make measurements in the far field of the HPM source. In either type of application (reception or transmission) with electrically large antennas, near-field measurement techniques need to be extended from the frequency domain [7] to the time domain [8]. In this report, we consider the calculation of the transient far-field response of an antenna from near-field data taken in either the time domain or the frequency domain.

The organization of this report is as follows. Section 2 considers the theory of the calculation of transient far fields from planar near-field data in either the time domain or the frequency domain. Section 3 illustrates the techniques with two idealized analytical examples. Section 4 explores the possibility of obtaining complex resonances of the antenna from near-field data via SEM. Section 5 summarizes the results of this study and includes recommendations for future work.

## 2. PLANAR NEAR-FIELD SCANNING

In this section we derive expressions for the far-field transient response of an antenna in terms of near-field values measured over a planar surface. The near-field values can be taken in either the frequency domain as in section 2.1 or the time domain as in section 2.2. We include no probe correction for pattern effects or frequency response; thus we assume that we can measure the electric field at any point on a plane for any frequency or any time. The results will be given in terms of two-dimensional integrals over a planar surface, but the integrals can be put in discrete form if evaluation by fast Fourier transform (FFT) is desired.

### 2.1 Frequency-Domain Approach

We first consider the time-harmonic case where the fields vary as $\exp(j\omega t)$. The geometry for planar scanning is shown in figure 1. An arbitrary antenna under test (AUT) is located in free space to the left of the plane $z = d$, and the values of the electric field $\mathbf{E}(\omega,\mathbf{r}')$ are measured on the plane $z = d$. An expression for the electric field $\mathbf{E}(\omega,\mathbf{r})$ for $z > d$ is available from Harrington [9, p. 111]

$$\mathbf{E}(\omega,\mathbf{r}) = \nabla \times \iint_{S'} \frac{e^{-jkR}}{2\pi R} \hat{z} \times \mathbf{E}(\omega,\mathbf{r}')\, dS', \tag{1}$$

where $R = |\mathbf{R}|$, $\mathbf{R} = \mathbf{r} - \mathbf{r}'$, $k = \omega/c$, $c$ is the speed of light in free space, and $\hat{}$ indicates a unit vector. The S' integration is over the plane $z = d$. If we take the curl operation inside the integral and carry out some algebra, then (1) becomes

$$\mathbf{E}(\omega,\mathbf{r}) = \iint_{S'} \frac{e^{-jkR}}{2\pi} \left(\frac{jk}{R} + \frac{1}{R^2}\right) [\hat{z} \times \mathbf{E}(\omega,\mathbf{r}')] \times \hat{R}\, dS'. \tag{2}$$

In the far field ($kr >> 1$, where $r = |\mathbf{r}|$), we can approximate $R$ by $r$ in amplitude terms and $R$ by $r - \hat{r} \cdot \mathbf{r}'$ in the phase. If we make these approximations in (2) and neglect the $r^{-2}$ term, then (2) reduces to

$$\mathbf{E}(\omega,\mathbf{r}) = -\frac{jke^{-jkr}}{2\pi r} \hat{r} \times \iint_{S'} \hat{z} \times \mathbf{E}(\omega,\mathbf{r}')\, e^{jk\hat{r}\cdot\mathbf{r}'}\, dS'. \tag{3}$$

The far-field result in (3) is equivalent to the expression given by Johnson [10, p. 332].

The Fourier transform nature of (3) is more evident if we write $\hat{r}$ in terms of polar angles $\theta$ and $\phi$ and $\mathbf{r}'$ in terms of rectangular coordinates:

$$\begin{aligned} \hat{r} &= \hat{x} \sin\theta \cos\phi + \hat{y} \sin\theta \sin\phi + \hat{z} \cos\theta \\ \text{and } \mathbf{r}' &= \hat{x}\, x' + \hat{y}\, y' + \hat{z}\, d. \end{aligned} \tag{4}$$

If we substitute (4) into the exponent and the differential in (3), we obtain

$$E(\omega,\mathbf{r}) = -\frac{jke^{-jk(r - d\cos\theta)}}{2\pi r}\,\hat{\mathbf{r}} \times \iint_{-\infty}^{\infty} \hat{\mathbf{z}} \times E(\omega,\mathbf{r}') \cdot$$

$$\cdot\, e^{jk\sin\theta(x'\cos\phi + y'\sin\phi)}dx'dy'. \tag{5}$$

If we wish to know the transient far-field response of the AUT, then we consider the far-field response in (3) or (5) to represent only one spectral component of the total transient response. The transient far-field response $\tilde{E}(t,\mathbf{r})$ is given by the inverse Fourier transform of $E(\omega,\mathbf{r})$:

$$\tilde{E}(t,\mathbf{r}) = F^{-1}[E(\omega,\mathbf{r})] = \frac{1}{2\pi}\int_{-\infty}^{\infty} E(\omega,\mathbf{r})\, e^{j\omega t}\, d\omega. \tag{6}$$

The evaluation of (6) involves a triple integral over x', y', and $\omega$. If we require $N_x$ samples in x', $N_y$ samples in y', and $N_\omega$ samples in $\omega$, then the total number of samples required would be $2N_xN_yN_\omega$. The factor of 2 arises because both tangential components (x and y) are required. The samples could be obtained either by sweeping (or stepping) through frequency $\omega$ at each near-field point or by doing a complete near-field scan at each frequency. Either method appears to be very time-consuming for typical values of $N_x$, $N_y$, and $N_\omega$. The evaluation of the triple integral does not appear to pose any particular problem because each integral is of the type that can be evaluated by FFT. Thus (6) could be evaluated by one three-dimensional FFT to obtain a grid of values of $\tilde{E}$ in $\theta$, $\phi$, and t.

## 2.2 Time-Domain Approach

In the time-domain approach, the AUT has a transient excitation, and the measured field values on the plane S' are functions of time $\tilde{E}(t,\mathbf{r}')$. We could derive an expression for $\tilde{E}(t,\mathbf{r})$ in terms of values of $\tilde{E}(t,\mathbf{r}')$ directly in the time domain, but it is easier to derive $\tilde{E}(t,\mathbf{r})$ from (3) and (6). The jk factor in (3) transforms as a time derivative, and the exponentials in (3) transform as time shifts. Thus (6) can be rewritten in the following form

$$\tilde{E}(t,r) = \frac{-1}{2\pi rc}\, \hat{r} \times \iint_{S'} \hat{z} \times \frac{\partial}{\partial t} \tilde{E}(t - \frac{r - \hat{r}\cdot r'}{c}, r')\, dS'. \tag{7}$$

In some cases, it is more convenient to use a shifted time, $\tau = t - r/c$, and to rewrite (7) as

$$\tilde{E}(t,r) = \frac{-1}{2\pi rc}\, \hat{r} \times \iint_{S'} \hat{z} \times \frac{\partial}{\partial t} \tilde{E}(\tau + \frac{\hat{r}\cdot r'}{c}, r')\, dS'. \tag{8}$$

From (7) or (8) we see that the time derivative of **E** is required at each near-field point **r'**. Thus a time waveform would need to be measured and stored at each near-field point. If we require $N_t$ time samples at each near-field point, then the total number of samples required would be $2N_xN_yN_t$. As in the frequency domain case, this is a very large number of samples for typical values of $N_x$, $N_y$, and $N_t$. The time domain result in (7) or (8) requires evaluation of only a double integral rather than a triple integral, but the double integral is not of the form that can be evaluated by FFT. If the probe measures the value of $\tilde{E}$, then the time derivative of $\tilde{E}$ would have to be computed for evaluation of (7) or (8). (This could be done by finite difference.) However, some probes actually measure the time derivative of the electric field directly, and these probes are usually called D-dot sensors [11].

The results in this section have been given for the electric field, but the same equations apply for the magnetic field. There are also probes available for measuring the time derivative of the magnetic field, and these probes are usually called B-dot sensors [11].

## 3. ANALYTICAL EXAMPLES

In this section we study two idealized examples where we are able to determine the transient far field analytically from the planar near-field distribution. We consider a step function distribution over a rectangular aperture in section 3.1 and a step function distribution over a circular aperture in section 3.2. In each case we perform the analysis starting with either frequency-domain near fields via (5) and (6) or transient near fields via (8). Even though the examples are idealized, they illustrate the differences in the integrations that must be performed. The examples also illustrate that we can obtain identical far-field results either working entirely in the time domain or working in the frequency domain followed by an inverse Fourier transform.

### 3.1 Rectangular Aperture

We consider first the rectangular aperture geometry shown in figure 2 where we have set d = 0. The time-dependent electric field in the z = 0 plane is assumed to be a step function inside the a by b aperture and zero outside the aperture and is assumed to be x-polarized

$$\tilde{E}(t,r') = \hat{x}\, E_s\, U(t)\, p_a(x')\, p_b(y'), \tag{9}$$

where $p_a(x') = \begin{cases} 1, & |x'| \leq a \\ 0, & |x'| > a \end{cases}$,

U(t) is the unit step function, and $E_s$ is a real constant with units of V/m. We do not need to consider what type of antenna would actually produce such a field, but a step-excited aperture antenna is one possibility. For evaluation of (8), we need the time derivative of the electric field

$$\frac{\partial}{\partial t} E(t,r') = \hat{x}\, E_s\, \delta(t)\, p_a(x')\, p_b(y'), \tag{10}$$

where $\delta(t)$ is a delta function [12]. If we substitute (10) into (8), we obtain the following expression for the far field

$$\tilde{E}(t,r) = \frac{-E_s}{2\pi rc}\, \hat{r} \times \hat{y}\, I_\delta \ , \tag{11}$$

where $I_\delta = \int_{-b}^{b} \int_{-a}^{a} \delta[\tau + (x'\sin\theta\cos\phi + y'\sin\theta\sin\phi)/c]\, dx'\, dy'$

and $\hat{r} \times \hat{y} = -\hat{x}\cos\theta + \hat{z}\sin\theta\cos\phi.$

For arbitrary $\theta$ and $\phi$, (11) can be evaluated, but the result is rather involved. The results simplify in the two principal planes ($\phi = 0$ or $\pi/2$). For $\phi = 0$, we have

$$\tilde{E}(t,r)\Big|_{\phi=0} = \hat{\theta}\, \frac{E_s b}{\pi r \sin\theta}\, p_{T_a}(\tau) \ , \tag{12}$$

where $T_a = (2a\sin\theta)/c.$

For $\phi = \pi/2$, we have a similar result

$$\tilde{E}(t,r)\Big|_{\phi=\pi/2} = \hat{x}\, \frac{E_s a\cos\theta}{\pi r \sin\theta}\, p_{T_b}(\tau), \tag{13}$$

where $T_b = (2b\sin\theta)/c.$

Both (12) and (13) are indeterminate for the on-axis case ($\theta = 0$). By taking the limit as $\theta$ approaches zero in (11), (12), or (13), we obtain

$$\tilde{E}(t,r)\Big|_{\theta=0} = \hat{x}\, \frac{2abE_s}{\pi rc}\, \delta(\tau). \tag{14}$$

Thus the far field for the on-axis case ($\theta = 0$) is proportional to aperture area times the time derivative of the aperture field. In figure 3, we show the two principal plane results. In either case as $\theta$ approaches zero, the pulse narrows and approaches a delta function as indicated by (14).

We now treat the same rectangular aperture example starting with frequency-domain values in the z = 0 plane. The frequency-domain values are obtained by taking the inverse Fourier transform of (9)

$$E(\omega,\mathbf{r}') = \hat{\mathbf{x}} \frac{E_s}{j\omega} p_a(x') \, p_b(y') \, , \tag{15}$$

where we have used the inverse transform of the unit step [12]. The far field is obtained by substituting (15) into (5)

$$E(\omega,\mathbf{r}) = \frac{E_s e^{-jkr}}{2\pi r c} \hat{\mathbf{r}} \times \hat{\mathbf{y}} \, I_e \, , \tag{16}$$

where $I_e = \int_{-b}^{b} \int_{-a}^{a} e^{jk\sin\theta(x'\cos\phi + y'\sin\phi)} \, dx' \, dy'$.

The double integration in (16) can be performed to yield

$$E(\omega,\mathbf{r}) = \frac{-2abE_s e^{-jkr}}{\pi r c} \hat{\mathbf{r}} \times \hat{\mathbf{y}} \frac{\sin(ka\sin\theta\cos\phi)}{ka\sin\theta\cos\phi} \frac{\sin(kb\sin\theta\sin\phi)}{kb\sin\theta\sin\phi} \, . \tag{17}$$

This is the general frequency-domain, far-field result, but it simplifies considerably for the principal-plane ($\phi = 0$ or $\pi/2$) or the on-axis ($\theta = 0$) special cases

$$E(\omega,\mathbf{r})\Big|_{\phi=0} = \hat{\theta} \frac{2abE_s e^{-jkr}}{\pi r c} \frac{\sin(ka\sin\theta)}{ka\sin\theta} \, , \tag{18}$$

$$E(\omega,\mathbf{r})\Big|_{\phi=\pi/2} = \hat{\mathbf{x}} \frac{2abE_s e^{-jkr}\cos\theta}{\pi r c} \frac{\sin(kb\sin\theta)}{kb\sin\theta} \, , \tag{19}$$

and $$E(\omega,\mathbf{r})\Big|_{\theta=0} = \hat{\mathbf{x}} \frac{2abE_s e^{-jkr}}{\pi r c} \, . \tag{20}$$

To obtain the transient far-field response from the frequency-domain far-field response, we use the inverse transform relationship in (6). It is possible to take the inverse transform of the general frequency-domain expression in (17), but the result is rather involved. For simplicity we consider the special cases in (18)-(20). The simplest case is the on-axis case ($\theta = 0$):

$$F^{-1}[E(\omega,r)\Big|_{\theta=0}] = \hat{x}\,\frac{2abE_s}{\pi rc}\,\delta(\tau)\ . \tag{21}$$

This result is in agreement with the direct time-domain result in (14). To take the inverse transform of (18) or (19), we need the following inverse transform [12]

$$F^{-1}[\frac{\sin(\omega T)}{\omega T}] \doteq \frac{p_T(t)}{2T}\ . \tag{22}$$

Using (22), we can transform the principal plane results in (18) and (19) to the time domain

$$F^{-1}[E(\omega,r)\Big|_{\phi=0}] = \hat{\theta}\,\frac{E_s b}{\pi r\sin\theta}\,p_{T_a}(\tau)\ , \tag{23}$$

$$\text{and } F^{-1}[E(\omega,r)\Big|_{\phi=\pi/2}] = \hat{x}\,\frac{E_s a\cos\theta}{\pi r\sin\theta}\,p_{T_b}(\tau)\ . \tag{24}$$

These results are in agreement with the direct time-domain results in (12) and (13).

### 3.2 Circular Aperture

We now consider a circular aperture geometry as shown in figure 4 where we have again set $d = 0$. The time-dependent electric field in the $z = 0$ plane is assumed to be a step function inside the circular aperture of radius A and zero outside the aperture and is assumed to be x-polarized

$$\tilde{E}(t,r') = \hat{x}\, E_s\, U(t)\, p_A(\rho') \ . \tag{25}$$

The time derivative of the electric field is

$$\frac{\partial}{\partial t}\, \tilde{E}(t,r') = \hat{x}\, E_s\, \delta(t)\, p_A(\rho') \ . \tag{26}$$

If we substitute (26) into (8), we obtain the following expression for the far field

$$\tilde{E}(t,r) = \frac{-E_s}{2\pi rc}\, \hat{r} \times \hat{y}\, I_A \ , \tag{27}$$

$$\text{where } I_A = \int_0^{2\pi} \int_0^{A} \delta\left[\tau + \frac{\rho'}{c} \sin\theta \cos(\phi'-\phi)\right] \rho'\, d\rho'\, d\phi'. \tag{28}$$

It is easy to see that $I_A$ is independent of $\phi$. The $\rho'$ integration can be performed using the properties of the delta function [12, p. 274], and the $\phi'$ integration can then be performed to yield the following result

$$\tilde{E}(t,r) = \frac{-AE_s}{\pi r \sin\theta}\, \hat{r} \times \hat{y}\, \frac{(T_A^2 - \tau^2)^{1/2}}{T_A}\, p_{T_A}(\tau) \ , \tag{29}$$

$$\text{where } T_A = \frac{A}{c} \sin\theta \ .$$

The waveform for the circular aperture case is shown in figure 5, and it differs from the rectangular aperture case because it does not have a step discontinuity. For the on-axis case ($\theta = 0$), the expression in (29) is indeterminate. If we take the limit as $\theta$ approaches zero, we obtain

$$\tilde{E}(t,r)\Big|_{\theta=0} = \hat{x}\, \frac{A^2 E_s}{2rc}\, \delta(\tau) \ . \tag{30}$$

The on-axis results for both the circular and rectangular apertures are proportional to the aperture area times the delta function.

We now treat the same circular aperture example starting with frequency-domain values in the z = 0 plane. The frequency-domain values are obtained by taking the inverse Fourier transform of (25)

$$E(\omega,r') = \hat{x}\,\frac{E_s}{j\omega}\,p_A(\rho') \ . \tag{31}$$

The far field is obtained by substituting (31) into (5)

$$E(\omega,r) = \frac{E_s e^{-jkr}}{2\pi rc}\,\hat{r} \times \hat{y}\,I_J \ , \tag{32}$$

$$\text{where } I_J = \int_0^{2\pi}\int_0^{A} e^{jk\rho'\sin\theta\cos(\phi'-\phi)}\,\rho'\,d\rho'\,d\phi' \ .$$

The integrations can be performed using the integral representation of the Bessel function [13], and we obtain a result which is equivalent to that of Johnson [10, p. 333]

$$E(\omega,r) = \frac{-A^2 E_s e^{-jkr}}{rc}\,\hat{r} \times \hat{y}\,\frac{J_1(kA\sin\theta)}{kA\sin\theta} \ , \tag{33}$$

where $J_1$ is the first-order Bessel function [13]. For the on-axis case, (33) simplifies to

$$E(\omega,r)\Big|_{\theta=0} = \hat{x}\,\frac{A^2 E_s e^{-jkr}}{2rc} \ . \tag{34}$$

To obtain the transient far field from the frequency-domain far field, we use the inverse transform relationship in (6). The necessary inverse transform of $J_1$ is given in [14, p. 300], and the time-domain field is

$$F^{-1}[E(\omega,r)] = \frac{-AE_s}{\pi r \sin\theta}\, \hat{r} \times \hat{y}\, \frac{(T_A^2 - \tau^2)^{1/2}}{T_A}\, p_{T_A}(\tau) \;. \tag{35}$$

This result agrees with that obtained in the time domain in (29). The on-axis result is obtained from the inverse transform of (34)

$$F^{-1}[E(\omega,r)\Big|_{\theta=0}] = \frac{A^2 E_s}{2rc}\, \delta(\tau) \;. \tag{36}$$

This result is also in agreement with the direct time-domain result in (30).

## 4. SINGULARITY EXPANSION METHOD

A major difficulty in determining the far-field transient response of an antenna from near-field data is the large amount of data that must be taken (either $2N_xN_yN_\omega$ or $2N_xN_yN_t$ samples). It would be convenient if we could extract some useful information from data taken at a single near-field point or at the terminals of the AUT (either $N_\omega$ or $N_t$ samples). This type of data has been taken in the frequency domain at NBS in an attempt to characterize the out-of-band response of antenna arrays [6].

During the past 15 years, a great deal of work has been done in characterizing the transient responses of antennas and scatterers in terms of natural resonances. This general approach has been named the singularity expansion method (SEM), and a recent review paper by Baum [15] contains an extensive bibliography on the subject.

Under some conditions a scalar response $\tilde{f}(t)$ can be written as a sum of damped exponentials

$$\tilde{f}(t) = \sum_n (a_n e^{s_n t} + a_n^* e^{s_n^* t})\, U(t) \;, \tag{37}$$

where $s_n = \sigma_n + j\omega_n$ ,

$\omega_n$ is an angular frequency, $\sigma_n$ is a damping constant, and * denotes complex conjugate. The n summation contains an infinite number of terms, but a small number of terms is often sufficient except at early times. The terms appear in conjugate pairs so that $\tilde{f}(t)$ is real. Here $\tilde{f}(t)$ could represent a scalar component of the surface current or radiated field of the AUT. The coefficients $a_n$ of the exponential terms are functions of position and excitation, but the complex frequencies $s_n$ are characteristic of the antenna and are independent of position. Consequently, if we know $\tilde{f}(t)$ at any point, then we can attempt to determine the characteristic frequencies $s_n$ from that single waveform. There can be computational difficulties in such a procedure [15], but the Prony method [16] has been used by a number of investigators.

To work in the frequency domain, we take the Fourier transform of (37)

$$f(\omega) = F[\tilde{f}(t)] = \sum_n \left(\frac{a_n}{j\omega - s_n} + \frac{a_n^*}{j\omega - s_n^*}\right) . \tag{38}$$

Each term in (38) represents a first-order pole singularity in the complex frequency plane. In some cases there could be other types of singularities in the complex frequency plane [15], but the form in (38) has been used for most numerical work [17]. In sections 4.1 and 4.2, we discuss the possibilities of determining the complex resonances from frequency-domain measurements of the input reflection coefficient or the near field.

## 4.1 Input Reflection Coefficient

The input reflection coefficient Γ is a useful quantity in characterizing the out-of-band response of antennas because it is directly related to the mismatch loss [6]. However, the input admittance Y is more useful for SEM analysis because it has been shown to have the same complex poles as the surface current expansion [18]. Thus $Y(\omega)$ has the same form as (38) and can be used to obtain the complex resonances $s_n$.

If $\Gamma$ is measured as a function of frequency, then $Y(\omega)$ can be calculated from

$$Y(\omega) = Y_0 \frac{1 - \Gamma}{1 + \Gamma} , \tag{39}$$

where $Y_0$ is the characteristic admittance of the transmission line. Schaubert [19] has used a related expression to obtain complex resonances from time-domain data via Prony's method. Noise in the $Y(\omega)$ measurements will cause errors in the computed $s_n$ locations, and the general problem of determining the pole locations from noisy frequency-domain data has been studied by Ksienski and Willis [17]. The number of poles that can be extracted from the frequency-domain data is limited by the quality of the data.

4.2 Near-Field Data

Near-field data is also a good indicator of the out-of-band response of antennas because it relates to both the radiating and impedance mismatch properties of the antenna [6]. If $E_\alpha(\omega, \mathbf{r}_m)$ is a scalar component of the electric field measured at a frequency $\omega$ and at a location $\mathbf{r}_m$, then we can write $E_\alpha$ in the SEM form of (38)

$$E_\alpha(\omega,\mathbf{r}_m) = \sum_n \left(\frac{a_n}{j\omega - s_n} + \frac{a_n^*}{j\omega - s_n^*}\right) . \tag{40}$$

The usual procedure would be to take swept-frequency measurements of $E_\alpha$ at a single near-field point $\mathbf{r}_m$ and to calculate the $s_n$ values based on that data set. However, if we take swept-frequency data at several $\mathbf{r}_m$ points, then we would have several data sets to use in the determination of the $s_n$ values, and we might expect to improve the accuracy or the number of $s_n$ values that can be determined. The use of multiple frequency-domain data sets for extraction of pole locations has been studied by Ksienski [20].

If we are only interested in a rough estimate of where the antenna response peaks in $\omega$, then there is probably no need to search for the poles in the complex frequency plane. The raw data $E_\alpha(\omega, r_m)$ will show peaks in $\omega$ [6]. Such peaks are sometimes used in estimating how many poles can be extracted from the data [21]. The SEM analysis of the data does appear to be attractive because the complex resonances of the AUT are independent of $r_m$. Hence the complex resonances ought to show up in the far-field response of the AUT.

## 5. CONCLUSIONS

The theory for calculating the transient far field of an antenna from planar near-field data has been developed. The near-field data can be in either the frequency domain or the time domain. For frequency-domain data, the required triple integral could be performed by a three-dimensional FFT. For time-domain data, only a double integral is required, but it is not of a form suitable for FFT.

Two analytical examples have been studied, and identical results are obtained starting with frequency-domain or time-domain data. The two examples, a step-function electric field over a rectangular or circular aperture, are idealized, but they illustrate the integrations that must be performed. In each case, the integrations can be done analytically.

The main difficulty in determining the transient far field from near-field data is the large amount of measured data ($2N_xN_yN_\omega$ or $2N_xN_yN_t$ samples) that must be taken. If time-domain or frequency-domain measurements are made at a single near-field point (or at the antenna terminals), then SEM might provide a means of determining the natural resonances of the antenna.

The theory presented in this report is preliminary, and a number of theoretical, numerical, and experimental extensions are possible. More theoretical work could be done on sampling and probe correction [7]. Other near-field scanning surfaces, such as spherical or cylindrical, could be considered. The examples in section 3 were chosen so that the integrations could be done analytically, but it would be useful to study some less idealized cases where the integrations would be done numerically. Such cases would allow sampling requirements to be studied numerically. Further experimental and computational work could involve SEM analysis of near-field data at a few near-field points or the complete near-field to far-field transformation. The question of what time-domain probes are most effective [8] also deserves further study.

## 6. REFERENCES


[1] Lind, W.R. Out of band performance of antennas. Moore School of Electrical Engineering Report No. 65-18; 1965.

[2] Levinson, D.S. Transmission-line measurement techniques. More Air Development Center Technical Report No. RADC-TR-65-187; 1965.

[3] Cown, B.J.; Cain, F.L.; Duffy, E.G. Statistical prediction model for EMC analysis of out-of-band phased array antennas. IEEE Trans. Electromag. Compat., EMC-18: 163-170; 1976.

[4] Cown, B.J.; Ryan, C.E.; Weaver, E.E. Antenna pattern measurements to characterize the out-of-band behavior of reflector antennas. Georgia Institute of Technology, Engineering Experiment Station, Report ECAC-TR-83-003; 1983.

[5] Hill, D.A. Out-of-band response of reflector antennas. Nat. Bur. Stand. (U.S.) Interagency Report 85-3021; 1985.

[6] Hill, D.A.; Francis, M.H. Out-of-band response of antenna arrays. Nat. Bur. Stand. (U.S.) Interagency Report 86-3047; 1986.

[7] Kerns, D.M. Plane-wave scattering-matrix theory of antennas and antenna-antenna interactions. Nat. Bur. Stand. (U.S.) Monograph 162; 1981.

[8] Lawton, R.A.; Ondrejka, A.R. Antennas and the associated time domain range for the measurement of impulsive fields. Nat. Bur. Stand. (U.S.) Tech. Note 1008; 1978.

[9] Harrington, R.F. Time-Harmonic Electromagnetic Fields. New York: McGraw-Hill; 1961.

[10] Johnson, C.C. Field and Wave Electrodynamics. New York: McGraw-Hill; 1965.

[11] Baum, C.E.; Breen, E.L.; Giles, J.C.; O'Neill, J.; Sower, G.D. Sensors for electromagnetic pulse measurements both inside and away from nuclear source regions. IEEE Trans. Antennas Propagat., AP-26: 22-35; 1978.

[12] Papoulis, A. The Fourier Integral and its Applications. New York: McGraw-Hill; 1962.

[13] Abramowitz, M.; Stegun, I.A., ed. Handbook of mathematical functions. Nat. Bur. Stand. (U.S.) Appl. Math Ser. 55; 1964 June.

[14] Roberts, G.E.; Kaufman, H. Table of Laplace Transforms. Philadelphia: W.B. Saunders Co.; 1966.

[15] Baum, C.E. The singularity expansion method: background and developments. IEEE Antennas & Propagation Society Newsletter, 28(4): 15-23; 1986.

[16] Van Blaricum, M.L.; Mittra, R. A technique for extracting the poles and residues of a system directly from its transient response. IEEE Trans. Antennas Propagat., AP-23: 777-781; 1975.

[17] Ksienski, D.A.; Willis, T.M. Numerical methods of noise reduction for frequency domain SEM. Electromagnetics. 4: 393-405; 1984.

[18] Pearson, L.W.; Wilton, D.R. Theoretical aspects of the physical realizability of broad-band equivalent circuits for energy collecting structures. IEEE Trans. Antennas Propagat., AP-29: 697-707; 1981.

[19] Schaubert, D.H. Application of Prony's method to time-domain reflectometer data and equivalent circuit synthesis. IEEE Trans. Antennas Propagat., AP-27: 180-184; 1979.

[20] Ksienski, D.A. Pole and residue extraction from measured data in the frequency domain using multiple data sets. Radio Science, 20: 13-19; 1985.

[21] Drachman, B.; Rothwell, E. A continuation method for identification of the natural frequencies of an object using a measured response. IEEE Trans. Antennas Propagat., AP-33: 445-450; 1985.

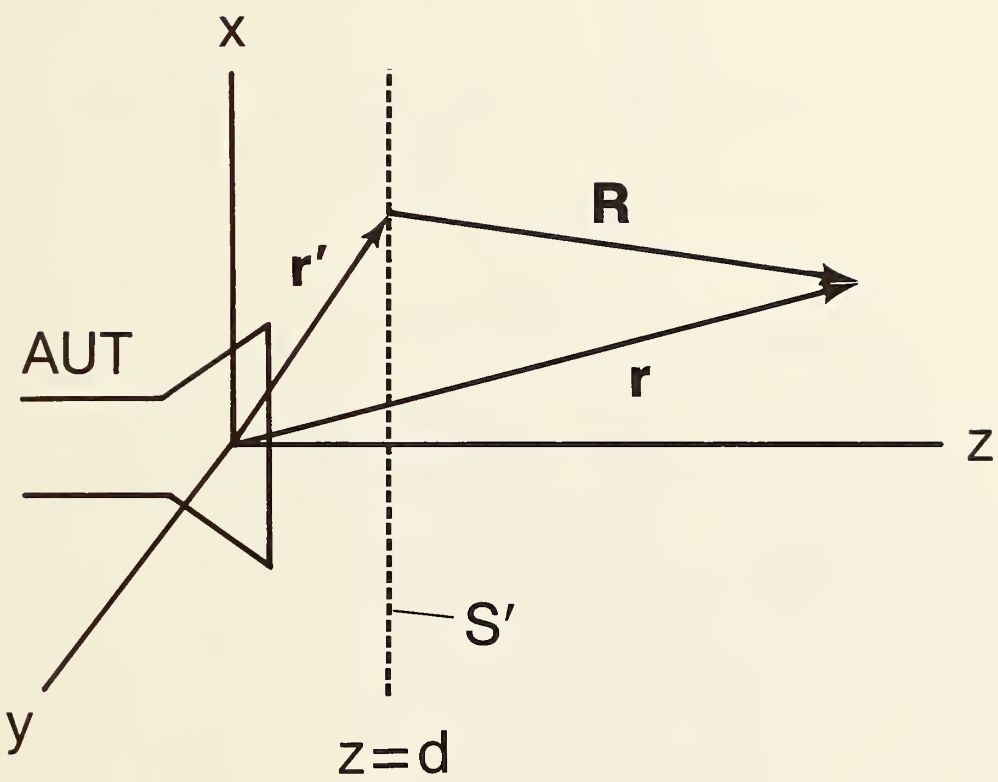


Figure 1. Near-field planar scanning geometry for an arbitrary antenna under test (AUT).

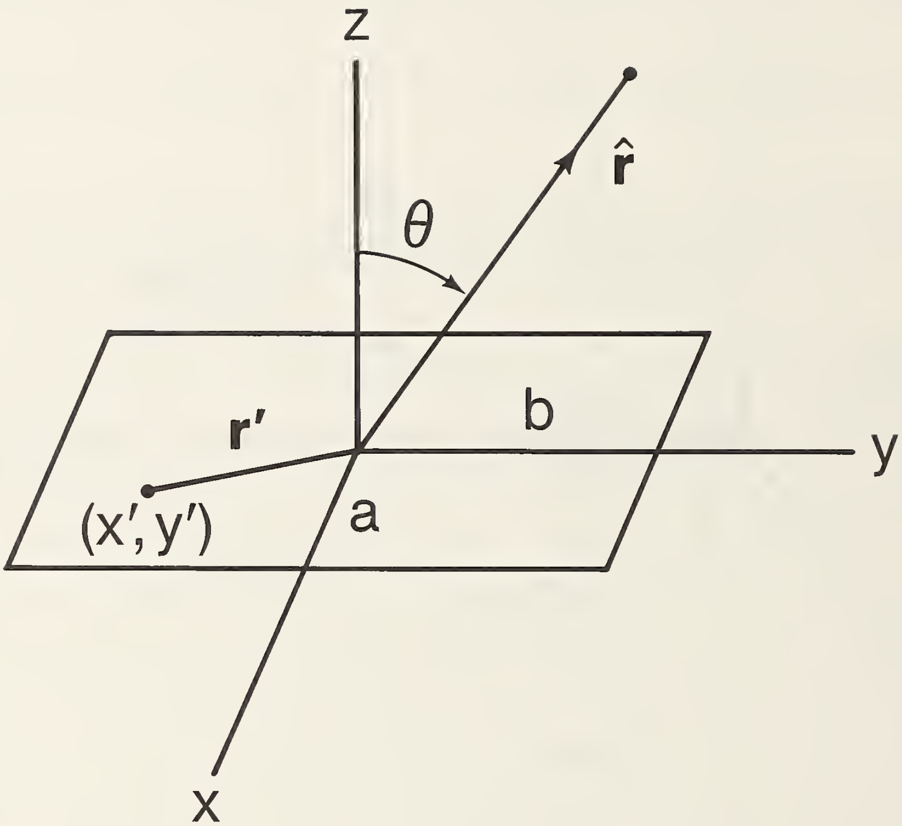


Figure 2. Rectangular aperture (2a x 2b).

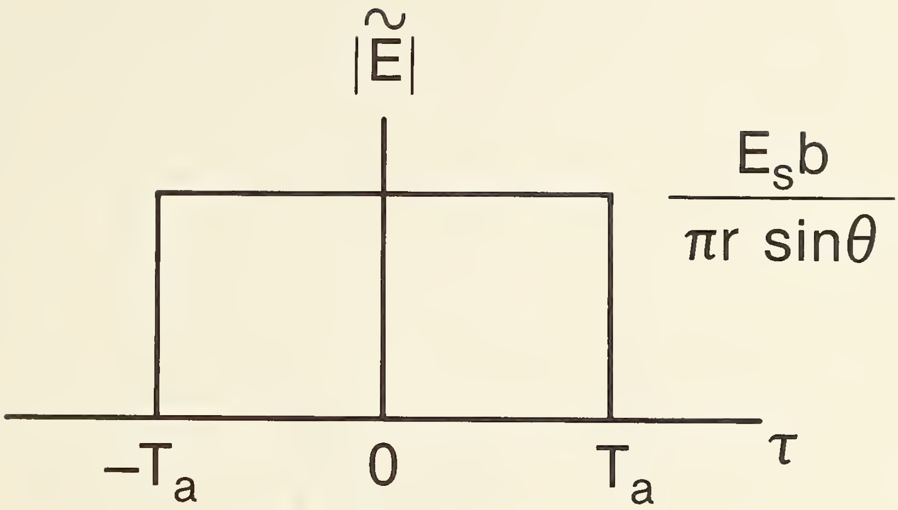


(a)

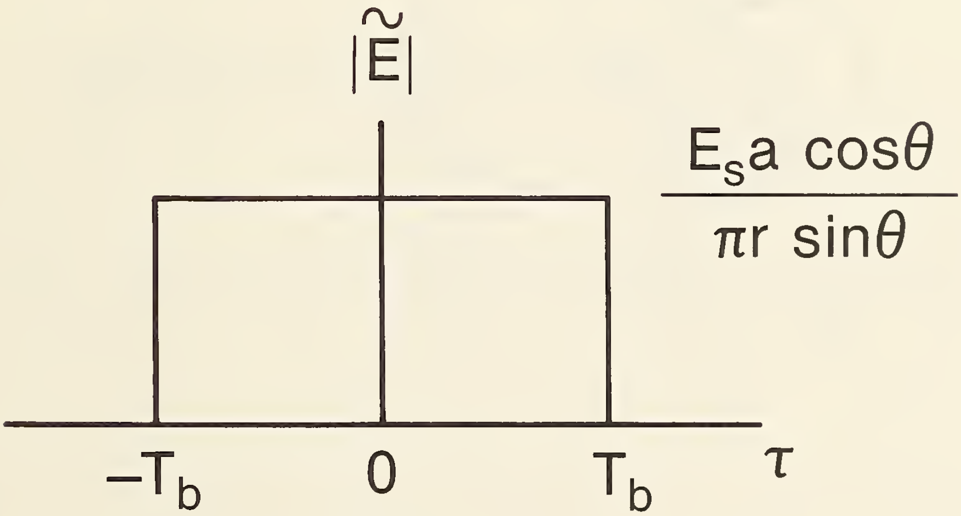


(b)

Figure 3. Time-dependent far field radiated by a rectangular aperture: a) $\phi$ = 0 plane, b) $\phi = \pi/2$ plane.

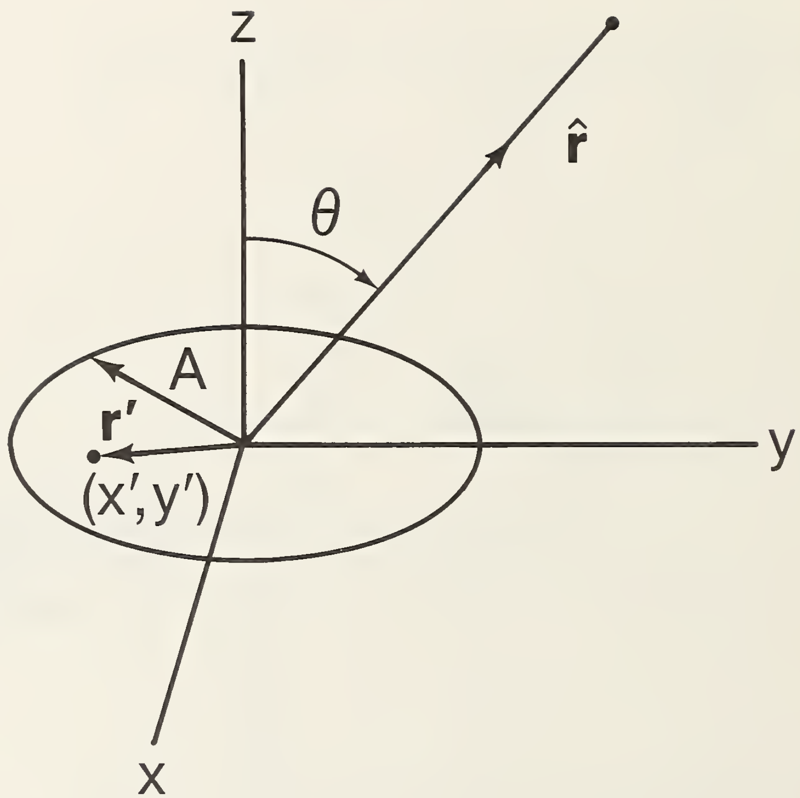


Figure 4. Circular aperture of radius A.

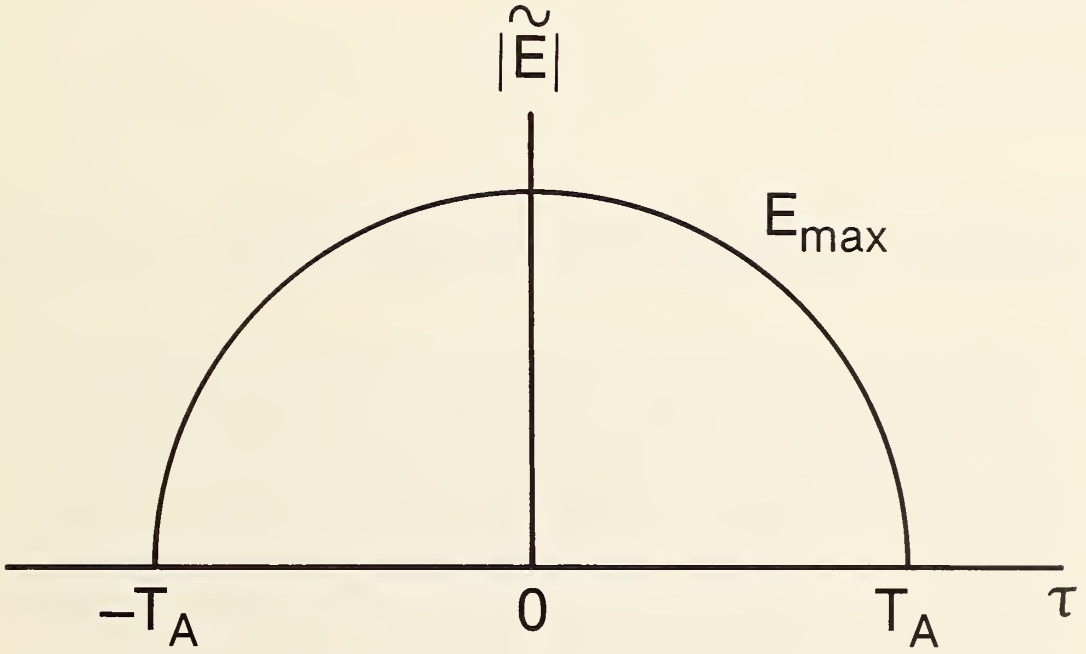


Figure 5. Time-dependent far field radiated by a circular aperture.

$E_{max} = |\hat{r} \times \hat{y}|\ AE_s/(\pi r \sin\theta)$.

NBS-114A (REV. 2-80)

| U.S. DEPT. OF COMM. BIBLIOGRAPHIC DATA SHEET (See instructions) | 1. PUBLICATION OR REPORT NO. NBSIR 86-3063 | 2. Performing Organ. Report No. | 3. Publication Date December 1986 |
|---|---|---|---|

4. TITLE AND SUBTITLE

Far-Field Transient Response of an Antenna From Near-Field Data

5. AUTHOR(S)

David A. Hill

6. PERFORMING ORGANIZATION (If joint or other than NBS, see instructions)

**NATIONAL BUREAU OF STANDARDS**
**DEPARTMENT OF COMMERCE**
**WASHINGTON, D.C. 20234**

7. Contract/Grant No.

8. Type of Report & Period Covered

9. SPONSORING ORGANIZATION NAME AND COMPLETE ADDRESS (Street, City, State, ZIP)

Defense Nuclear Agency
Alexandria, Virginia 22310

10. SUPPLEMENTARY NOTES

☐ Document describes a computer program; SF-185, FIPS Software Summary, is attached.

11. ABSTRACT (A 200-word or less factual summary of most significant information. If document includes a significant bibliography or literature survey, mention it here)

The theory for calculating the transient far-field response of an antenna from planar near-field data in either the time domain or the frequency domain has been developed. A double integral must be evaluated if we begin with time-domain data, but a triple integral must be evaluated if we begin with frequency-domain data. However, the frequency-domain integrals are in a form that is suitable for three-dimensional FFT. Two idealized examples are studied, and identical results are obtained starting with frequency-domain or time-domain data. The main practical difficulty in determining the transient response is the large number of near-field samples that are required. If data are taken at only a few near-field points, then the singularity expansion method (SEM) presents a possible method of determining the complex resonances of the antenna under test.

12. KEY WORDS (Six to twelve entries; alphabetical order; capitalize only proper names; and separate key words by semicolons)

antenna; complex resonance; far field; frequency domain; near field; singularity expansion method (SEM); time domain.

13. AVAILABILITY

☒ Unlimited
☐ For Official Distribution. Do Not Release to NTIS
☐ Order From Superintendent of Documents, U.S. Government Printing Office, Washington, D.C. 20402.
☒ Order From National Technical Information Service (NTIS), Springfield, VA. 22161

14. NO. OF PRINTED PAGES

28

15. Price